

Conf-941174--1

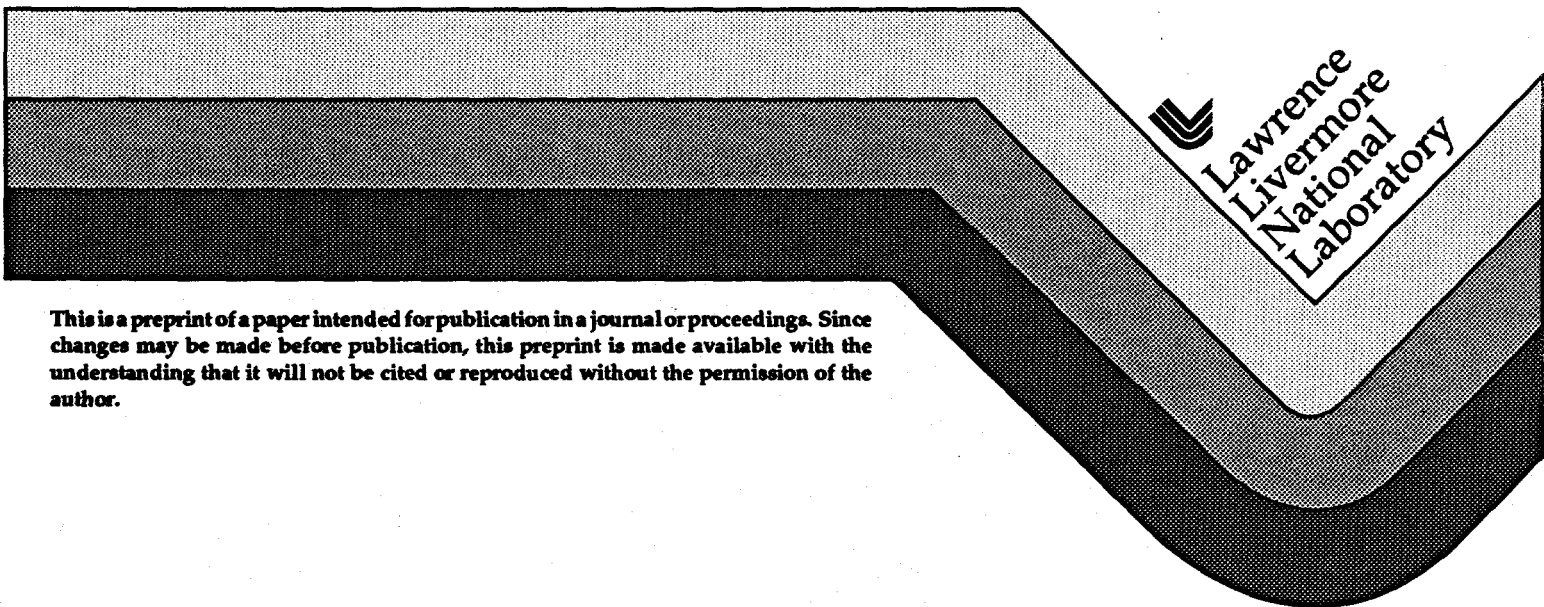
UCRL-JC-115959
PREPRINT

Laser-induced Fluorescence Diagnostic for the LEM Turbulent Hydrodynamics Experiment

B. Remington
G. Dimonte

This paper was prepared for submittal to the
1994 Division Dynamics Annual Conference
Atlanta, GA
November 20-22, 1994

December 1994



This is a preprint of a paper intended for publication in a journal or proceedings. Since changes may be made before publication, this preprint is made available with the understanding that it will not be cited or reproduced without the permission of the author.

DISCLAIMER

This document was prepared as an account of work sponsored by an agency of the United States Government. Neither the United States Government nor the University of California nor any of their employees, makes any warranty, express or implied, or assumes any legal liability or responsibility for the accuracy, completeness, or usefulness of any information, apparatus, product, or process disclosed, or represents that its use would not infringe privately owned rights. Reference herein to any specific commercial product, process, or service by trade name, trademark, manufacturer, or otherwise, does not necessarily constitute or imply its endorsement, recommendation, or favoring by the United States Government or the University of California. The views and opinions of authors expressed herein do not necessarily state or reflect those of the United States Government or the University of California, and shall not be used for advertising or product endorsement purposes.

DISCLAIMER

Portions of this document may be illegible in electronic image products. Images are produced from the best available original document.

Talk prepared for the
1994 Division of Fluid Dynamics Annual Conference
November 20-22, 1994, Atlanta, GA

Laser-induced Fluorescence Diagnostic for the LEM Turbulent Hydrodynamics Experiment*, Bruce Remington and Guy Dimonte, LLNL, Livermore, CA 94551. We are developing a laser-induced fluorescence (LIF) diagnostic for the LEM experiment¹ to measure the evolution of a Rayleigh-Taylor unstable fluid interface into the highly nonlinear regime. The interface will be between two fluids of different density in a 7 x 7 x 14 cm cell that will be accelerated downwards over a distance of ~100 cm, achieving maximum velocities of order 50 m/s. One of the two fluids will be doped with laser dye and pumped to fluoresce with a 100 Hz pulsed, frequency doubled YAG laser beam spread into a sheet and entering the cell from the bottom. The short pulse duration of the laser (<10 ns) eliminates motional blurring, and the images are recorded from the side with a series of 35 mm static cameras. Aligning the laser sheet to the center of the cell localizes the region of the cell probed and eliminates edge effects in the data. This LIF diagnostic will be described. *Work performed under the auspices of the U.S. Department of Energy by the Lawrence Livermore National Laboratory under contract number W-7405-ENG-48.

¹G. Dimonte *et al.*, companion poster.

DISTRIBUTION OF THIS DOCUMENT IS UNLIMITED

YD

MASTER

In Figure 1, I show a set of images in exposure from one of the dye concentration scaling runs. The brightness scale has been adjusted on each. A concentration of 250 $\mu\text{g/liter}$ of Kiton red corresponds approximately to 10^{-6} M molar concentration. In these images, the laser enters from the bottom, and there are two sets of ND step wedges at the bottom of the cell for film calibration. The camera used was our standard Ricoh with a Pentax 50 mm lens at F# 1.4 at a distance of 25 cm from the cell. The film was Tmax 400 and an OG550 filter was used to cut out any scattered green laser light. The laser was run in single-shot mode at the maximum allowed power (70 lamp joules/pulse) with a $\Delta t=20$ msec interval between shutting off repping and pulsing the single shot. Two features are apparent in these images. Looking at the bottom row (20, 2, 0.2 $\mu\text{g/liter}$), there is enhanced brightness on the axis of the camera. By aligning the camera to the top of the cell for the 20 $\mu\text{g/liter}$ case (092094b2.pds), we see that this enhancement follows the axis of the camera lens. Second, at the highest dye concentration (2000 $\mu\text{g/liter}$), there is clear pump depletion, that is, the laser light is diminished by the top of the cell, so that the image is brightest at the bottom.

In Fig. 2, I show the results from analyzing a dye concentration scaling run similar to that shown in Fig. 1. Figure 2a shows how I treat the film calibration. I use the lower row of ND steps, ND=0.1, 0.3, 0.5, 1.0, 2.0, 3.0, (a later set goes up to ND of 4.0), and compare a horizontal lineout through the center of the ND step wedge with a lineout just above it. By comparing the ΔFD (film density) with the known ΔE (exposure) based on the ND step, a film curve can be constructed. This has to be done in an iterative fashion, because the exposure of the upper (unattenuated) lineout is also changing from left to right due to the structure of the laser sheet. The film curve resulting from such an analysis for the 2000 $\mu\text{g/liter}$ cell is shown by the dotted curve and open circles in Fig. 2a. If a similar analysis is done for the 250 $\mu\text{g/liter}$ cell, one gets the solid curve. The 20

$\mu\text{g/liter}$ cell leads to the dashed curve. What is going on is that for the brightest cell (2000 $\mu\text{g/liter}$), one cannot reliably get the lowest values of FD vs exposure using the ND steps of 3.0 and 4.0. The finite spatial resolution of our system effectively "puts light under" the ND step. Hence, the final film curve is the composite of a bright, intermediate, and dim cell, that is, the dashed curve for $\text{FD} < 200$, solid curve for $200 < \text{FD} < 400$, and dotted curve for $\text{FD} > 400$. I have developed software that does this reasonably painlessly.

Figures 2b-2g are vertical lineouts showing exposure profiles through the center of the cell from bottom to top (bottom corresponds to zero) for the various dye concentrations. The camera was set up the same as in Fig. 1, i.e., Pentax lens at 25 cm from the cell, using F# 1.4. The two effects mentioned regarding the images shown in Fig. 1 dominate the analysis here. Figures 2b-2d are at low dye concentration, have negligible pump depletion, but show the pronounced peaking of exposure near the axis of the lens. Figures 1e-1g have the added effect of pump depletion. The pump depletion has been measured both with a power meter, and with images taken at higher F# (which will be discussed next in Fig. 3). At each dye concentration, a mean-free-path (MFP) is defined for the laser light, and the vertical lineout is corrected via

$$E_1(y) = E_0(y)/e^{-y/\text{MFP}}, \quad (1)$$

where y is the distance from the bottom of the cell. The dotted curves in Figs. 2d-2g show the results after this correction for pump depletion. Note that the dotted and solid curves are the same at $y=0$. For dye concentrations of 20 $\mu\text{g/liter}$ and less, this correction is negligible.

The set of dotted curves needs to include the flat field correction of the lens. In using a large aperture lens (F# 1.4, $f=50$ mm) at short object distances (25 cm) to look at a 14 cm high cell, one is covering angles of $\pm 15^\circ$ off the axis of the lens. Furthermore, the solid angle for light collection is dominated by the outer regions of the lens, where lens aberrations are the largest. Rays arriving at the lens far off axis are not brought to focus properly at the image plane by the outer regions of the lens. Hence, one gets this peaking along the axis of the lens. (At higher F#, this effect should be less.) I define a Gaussian flat field correction curve based on the dotted profile in Fig. 2d, and shown as the dotdashed curve. This curve is then scaled to compare with the rest of the dotted curves in Fig. 2. Other than a couple of aberrant cases near the very top of the cell, one can see

that a reasonable flat field correction can be done. The final, corrected lineout would be

$$E_2(y) = E_1(y)/e^{-(y-y_0)^2/2\sigma^2}, \quad (2)$$

where y_0 defines the axis of the lens, and σ represents the curvature being corrected for.

To deduce self-consistent values of exposure vs dye concentration, one does not need to do a full flat field correction. It should be sufficient to simply read off the peak values of exposure from the dotted curves in Fig. 2, that is, the values at $y=y_0$ and shown by the dashed lines. The exposure vs dye concentration curve can finally, then be generated. This is shown in a log-log plot in Fig. 2h, where we see a reasonable proportionality between dye concentration and exposure over 4 orders of magnitude. I would recommend that our standard running condition be with a cell with 100 $\mu\text{g/liter}$ dye concentration. Seeing mixing down to dilutions of 1/100th of nominal should be straight forward.

Figure 3 shows an identical analysis with the same lens only at F# of 5.6. Here, the peaking of exposure near the axis of the lens is negligible except at the highest dye concentration. The curve shown in Fig. 3c for 250 $\mu\text{g/liter}$ is taken as the standard for determining the MFP of the laser. Using Eq. 1, a value of the MFP is found so that the corrected curve is flat across the extent of the cell, shown by the dotted curve in Fig. 3c. The MFP was 46 cm here. This value is then scaled up and down for the other dye concentrations. The corresponding exposure vs dye concentration curve at F#=5.6 is shown in Fig. 3f. Due to the dimmer images at higher F#, the lowest observable exposure is at 2 $\mu\text{g/liter}$ concentration. But again, we have reasonable proportionality between exposure and dye concentration over 3 orders of magnitude.

Thinking that a macro lens is designed for close-in work and might have fewer lens aberration effects, we tried a Sigma macro lens at F#2.8. The distance to the cell was 16 cm. The results of that analysis are shown in Fig. 4. We must have a poor quality macro lens, because by comparison, these results are quite unsatisfactory.

Figure 5 shows the scaling of exposure with laser energy, as measured by light on the back side of one of the dichroic mirrors just past the KDP crystal. Other than an apparent low energy threshold, this scaling looks fine. We used a cell with 100 $\mu\text{g/liter}$ dye

concentration for this run so that only the lens flat field correction needed to be taken into account.

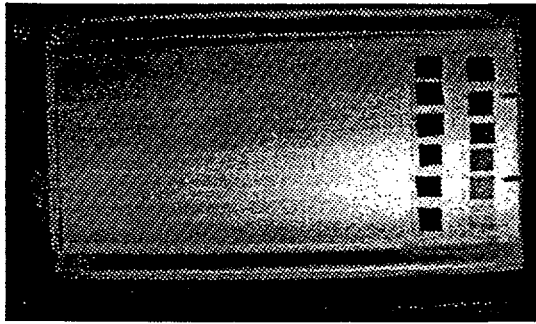
Figure 6 shows the exposure for the 250 $\mu\text{g/liter}$ cell at various z positions relative to $z=0$, that is, relative to the position of best focus in the thin dimension of the laser sheet. The results are shown at two F#'s (5.6 and 1.4), using our standard Pentax lens at 25 cm from the cell. For the range of z of +50 cm beyond best focus to -100 cm in front of best focus, we get $\text{FD} > 1.0$ at both F#'s, as shown in Fig. 6b. Provided we are careful with alignment, it appears that we may have some leeway in choosing F#. Figure 6c shows the loss of signal due to using F# 5.6 vs 1.4.

Figure 7 shows the degree to which the laser can be aligned to the axis of the LEM. We used a horizontal rail on the optical table as the LEM axis. After aligning the laser axis to this axis, we took direct images of the laser profile. The values plotted in Fig. 7 correspond to the centroid of the laser profile relative to the LEM axis both in rep mode (a) and in single-shot mode (b). It looks like with only a modest effort, we can align the laser axis to $\pm 1/2$ mm, which should be good enough for initial LEM experiments.

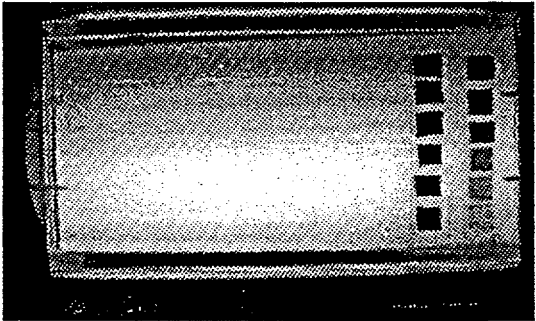
9_14_94_06,11,15,19,26,31: Exposure vs dye-concentration, fixed E_{Laser}



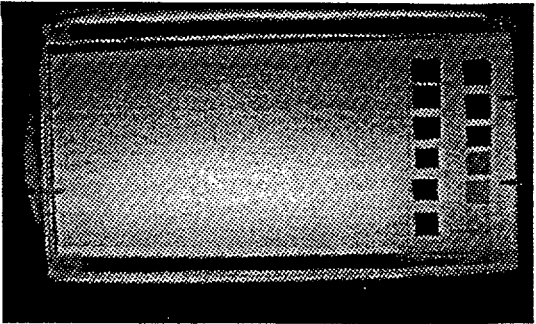
2000 $\mu\text{g/liter}$



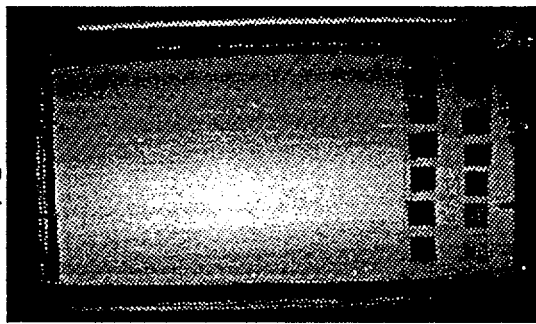
500 $\mu\text{g/liter}$



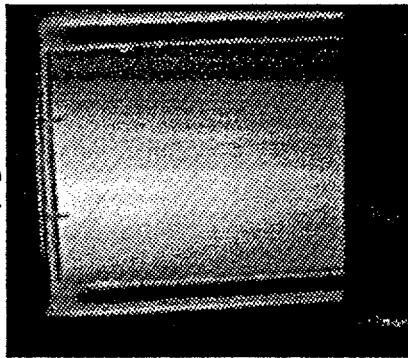
250 $\mu\text{g/liter}$



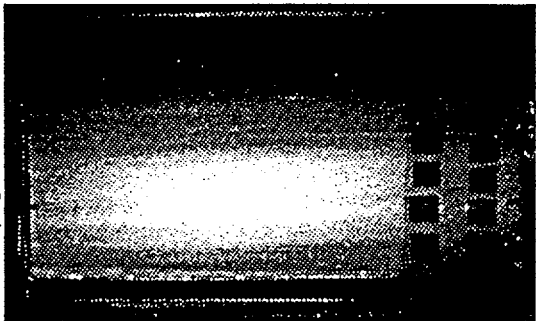
20 $\mu\text{g/liter}$



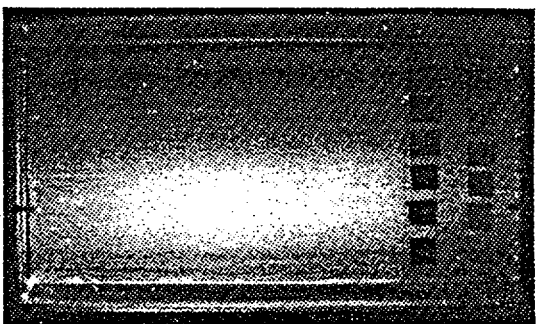
20 $\mu\text{g/liter}$



2 $\mu\text{g/liter}$



0.2 $\mu\text{g/liter}$



(092094b22.pds)

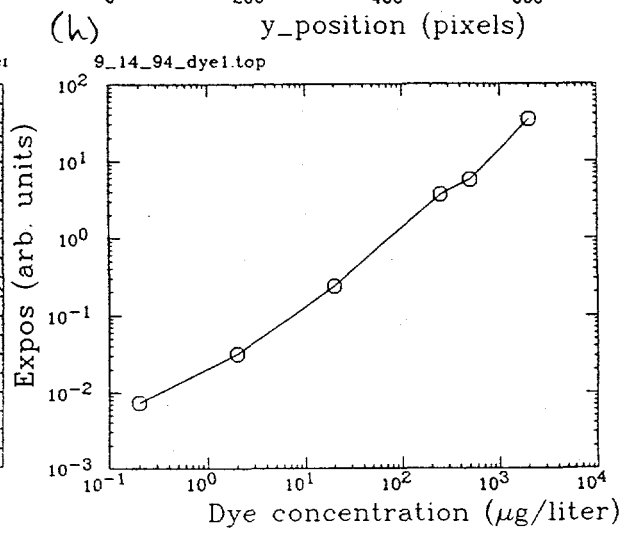
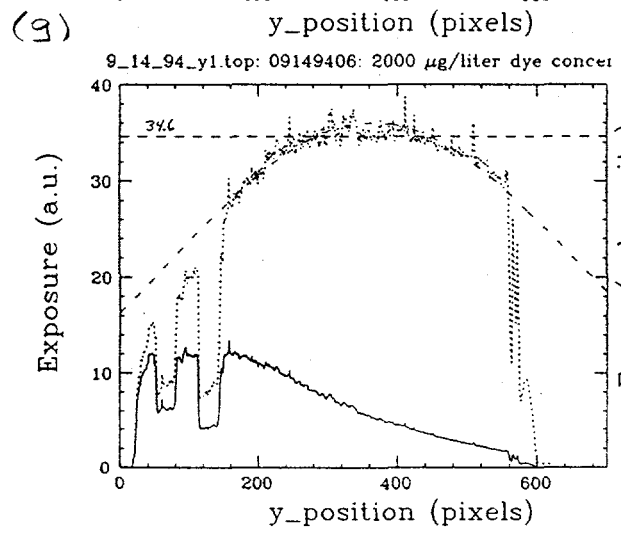
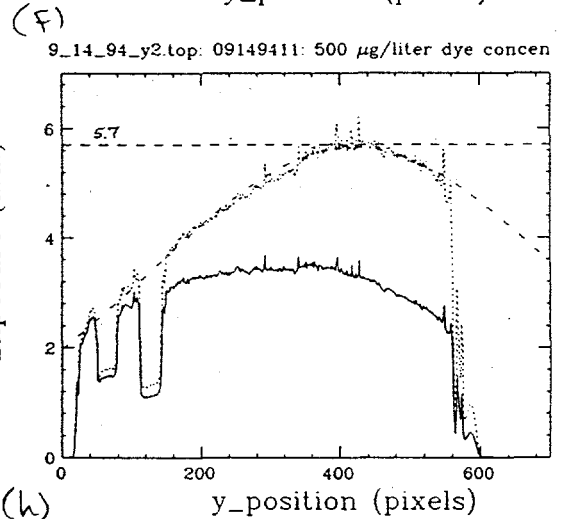
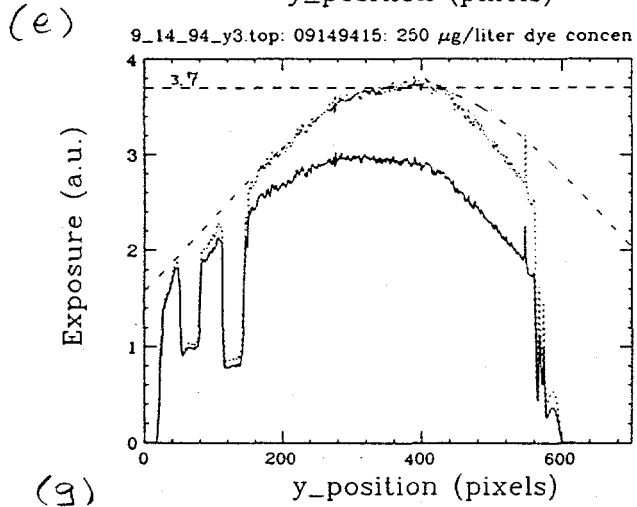
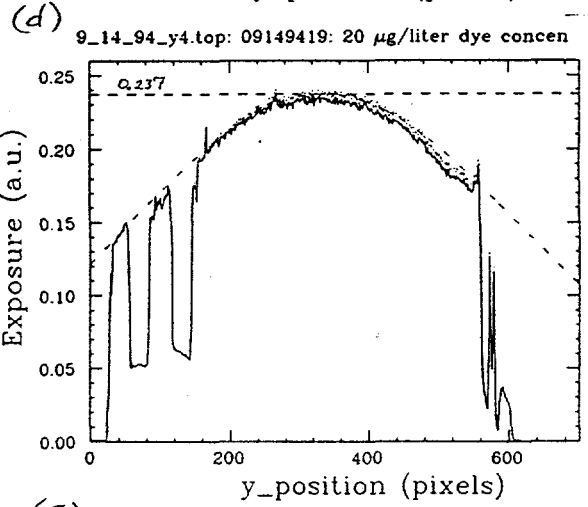
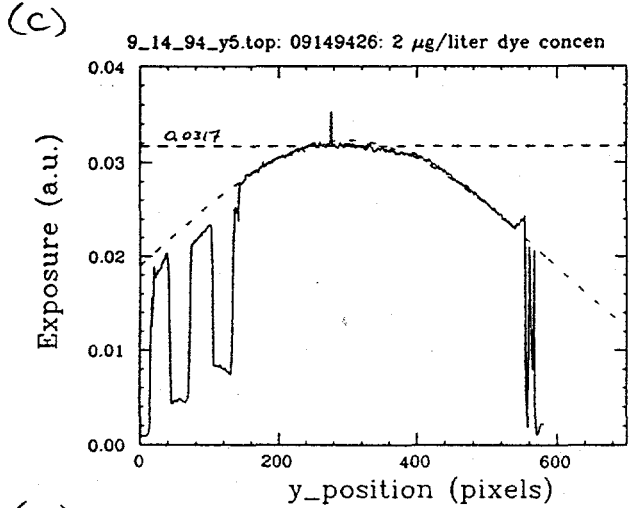
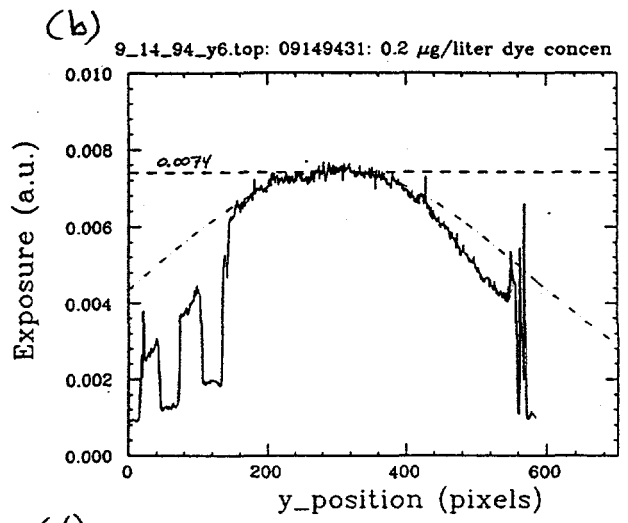
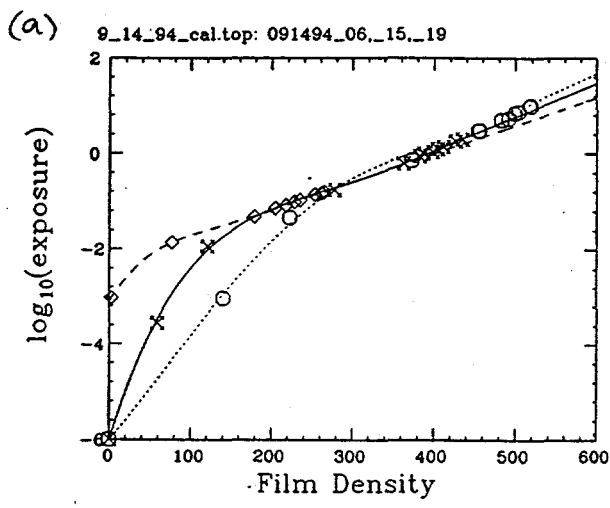


Fig. 2

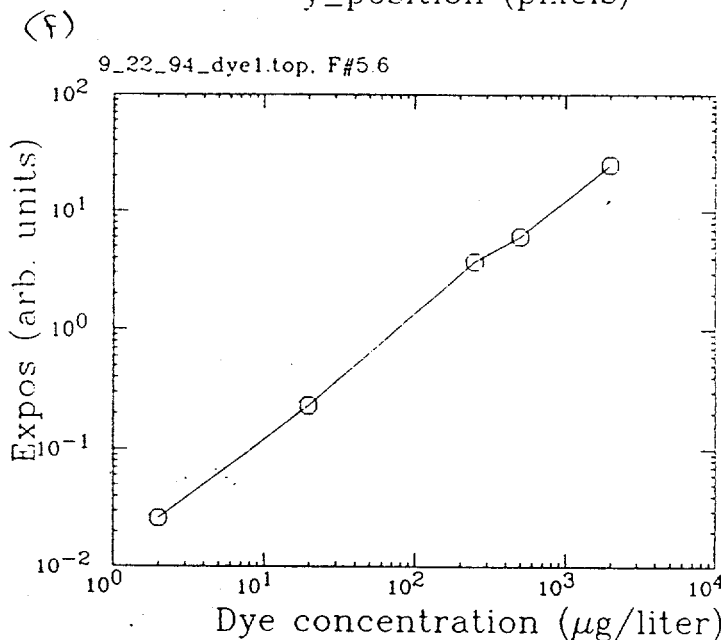
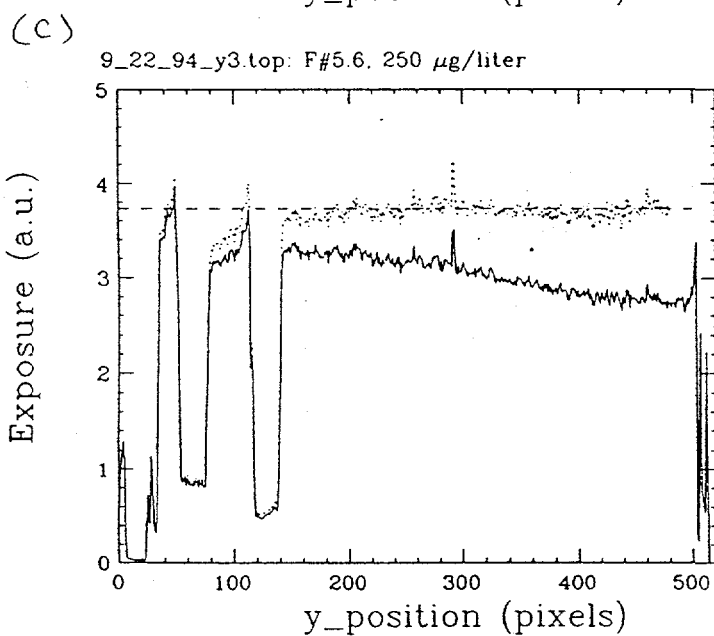
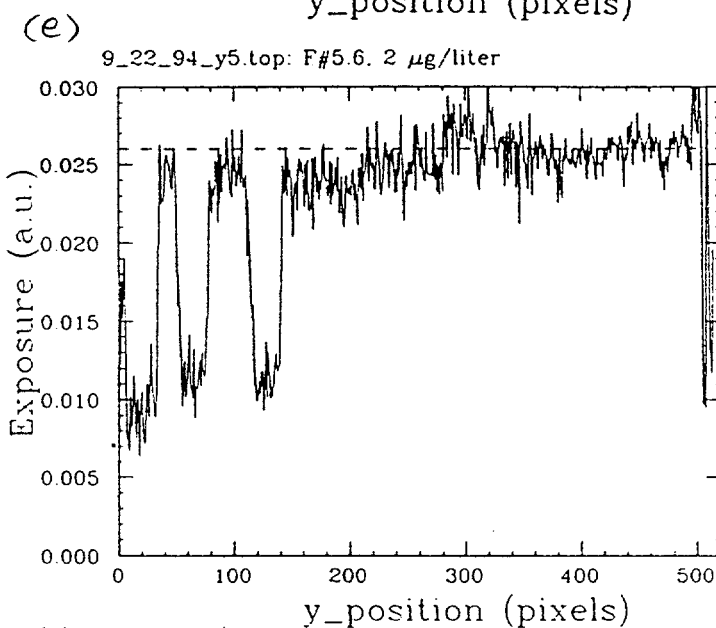
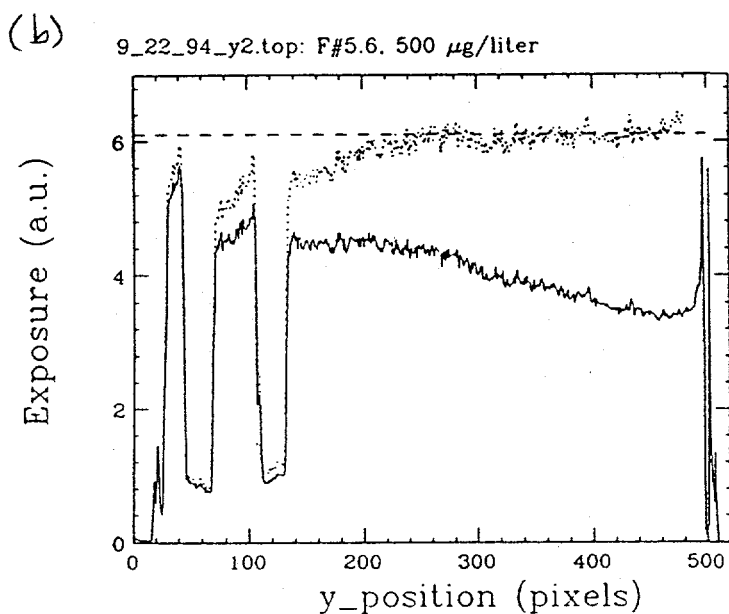
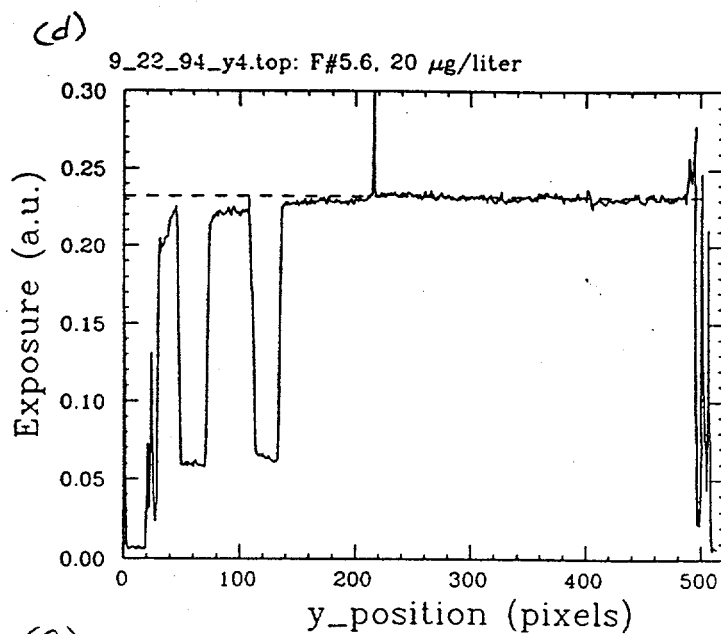
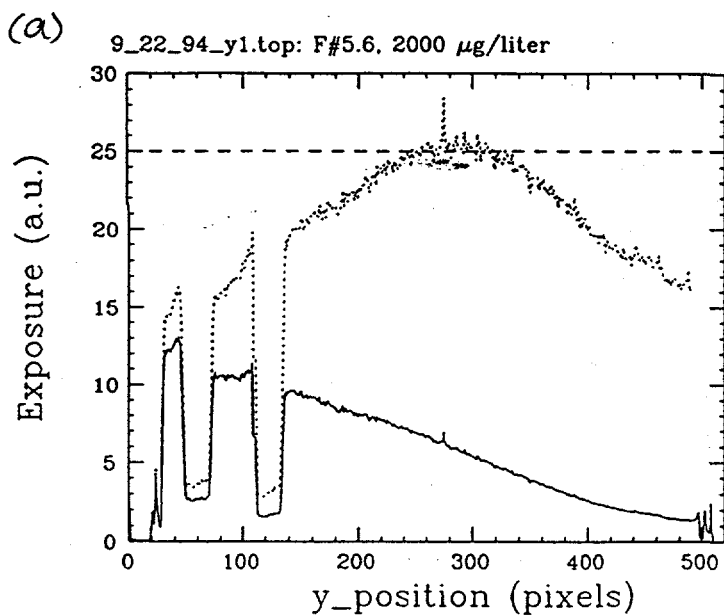


Fig. 3

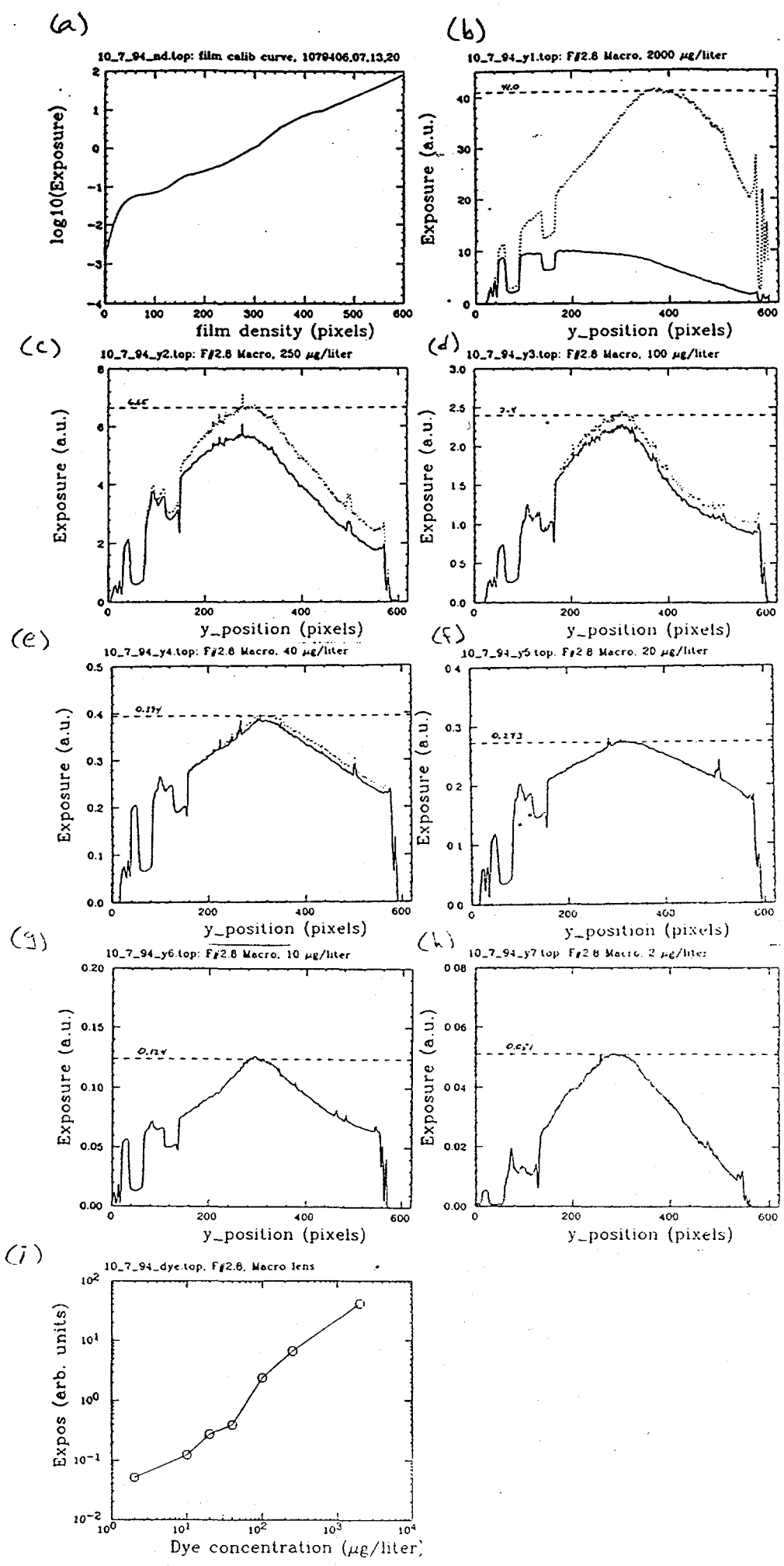
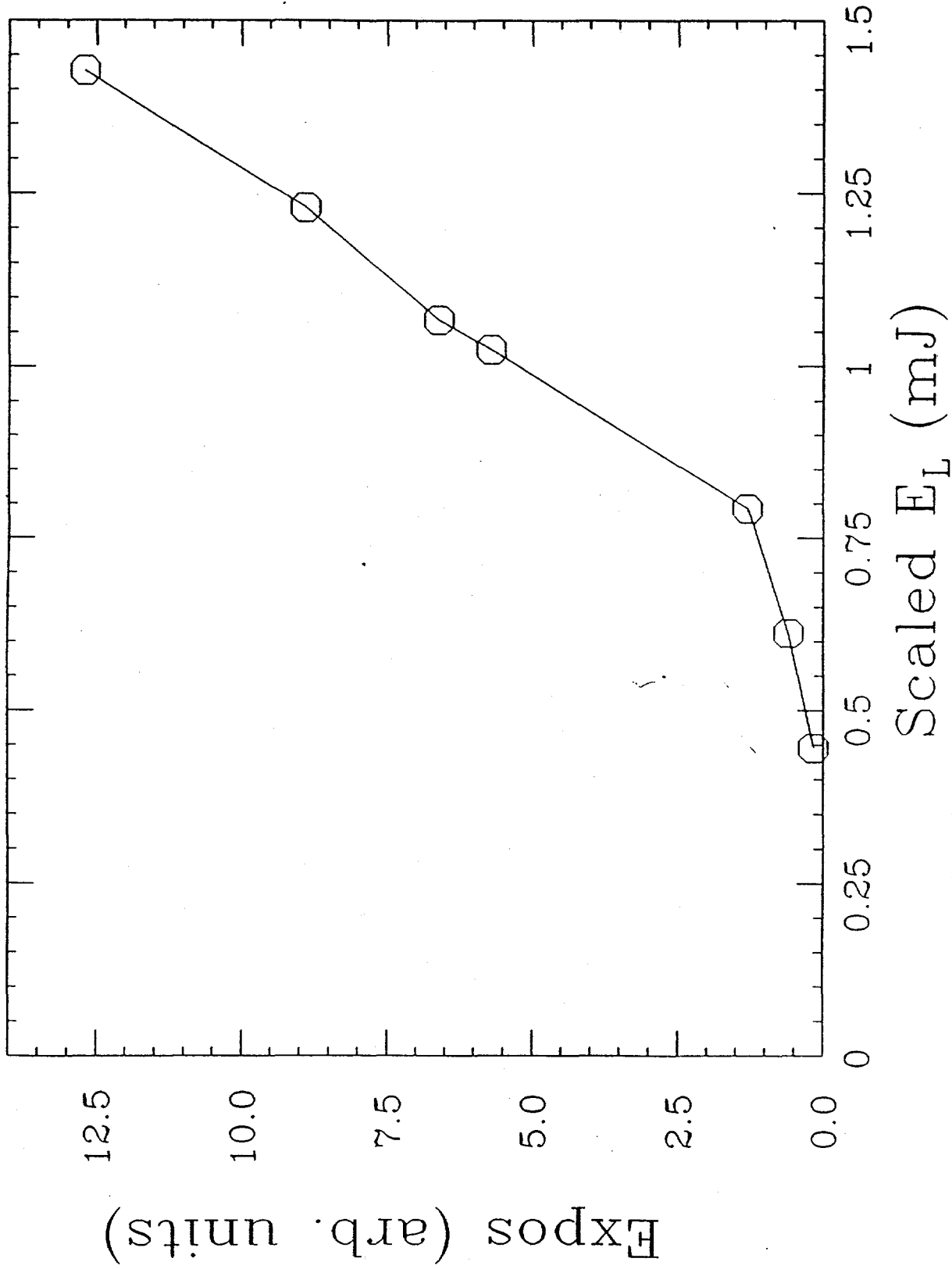


Fig. 4

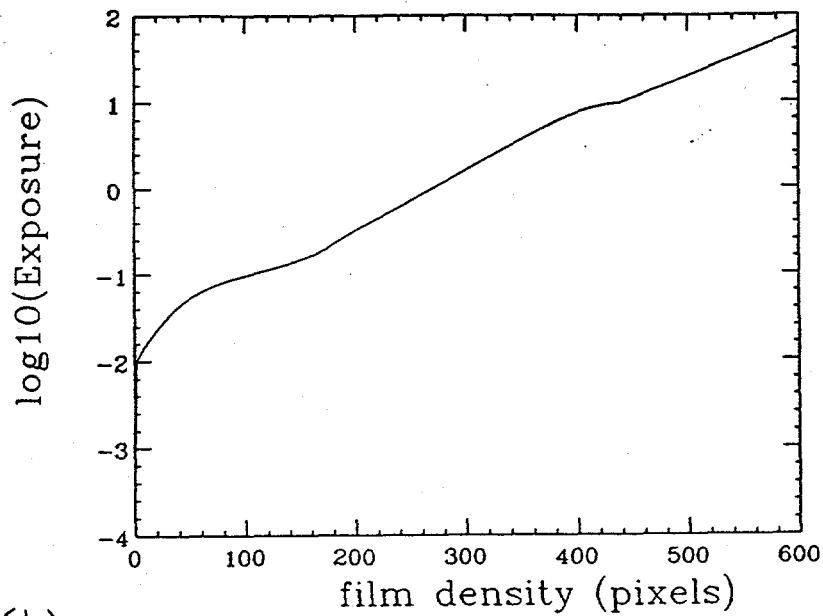
10_7¹⁰_94_EL.top, F#2.8, Macro lens, E_L scaling



*E_L measured at the back side of one of the
bichroic mirrors just past the KDP, pig. doubling crystal.*

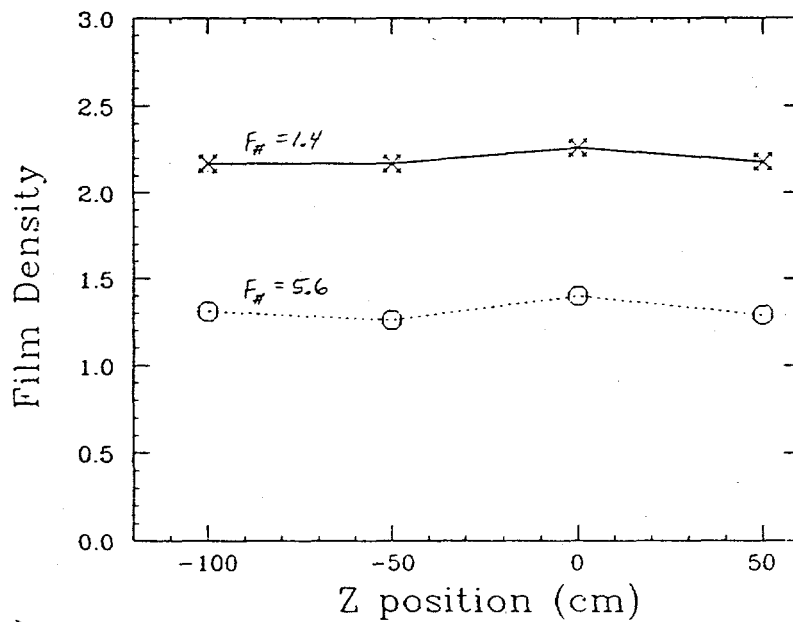
Fig. 5

(a) 9_27_94_nd.top: film calib curve, 09279409.29



(b)

9_27_94_z1.top: Max FD vs Z position, F#1.4,5.6



(c)

9_27_94_z.top: Max(Exposure) vs Z position, F#1.4,5.6

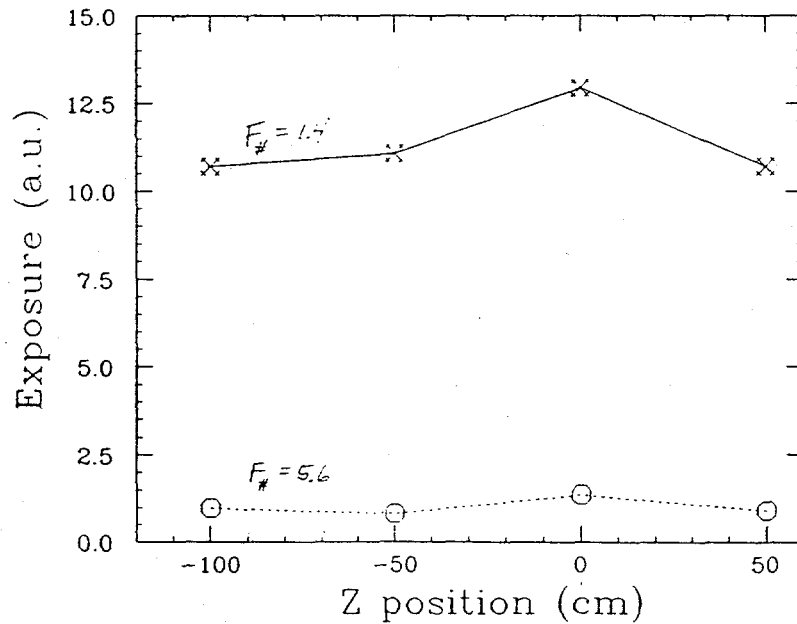
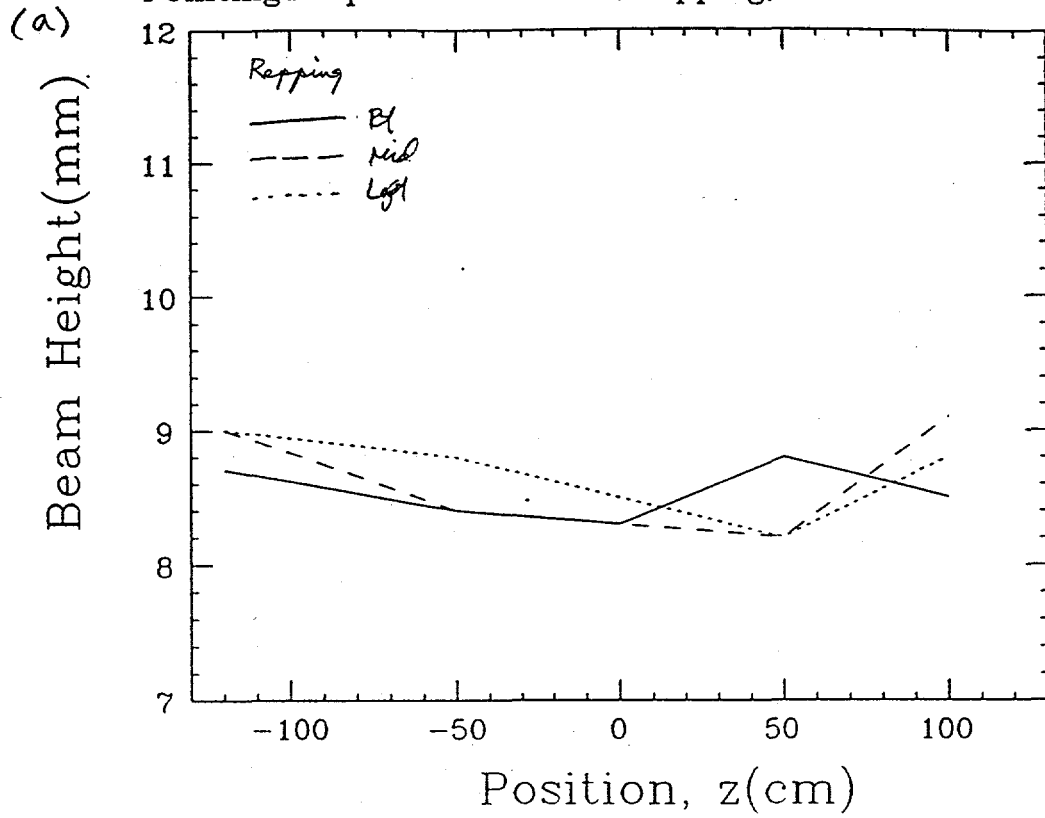
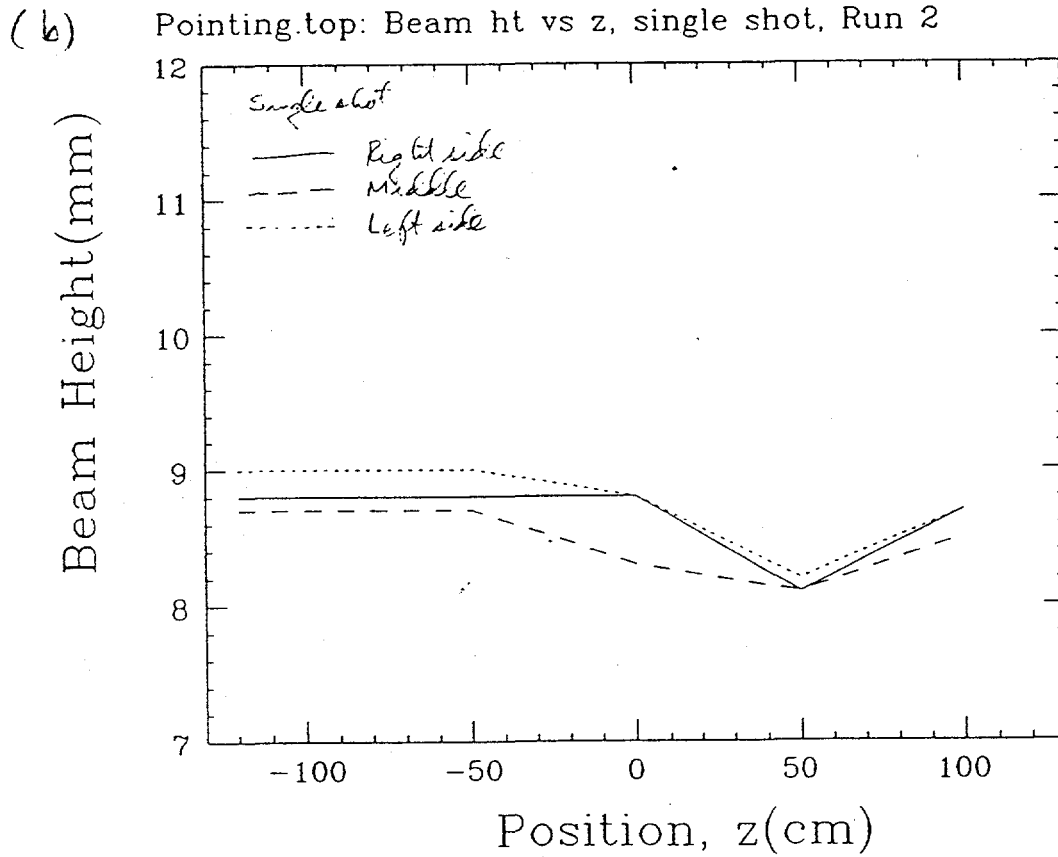


Fig. 6

Pointing1.top: Beam ht vs z, repping, Run 2



Pointing.top: Beam ht vs z, single shot, Run 2



We point to ~1mm accuracy ($\pm 1/2$ mm).